

# Impact of the DMRS Pattern on NR V2X Sidelink Communications

Luca Lusvardi, Baldomero Coll-Perales, Javier Gozalvez  
UWICORE Laboratory, Universidad Miguel Hernandez de Elche, Elche, Spain  
Email: {llusvardi, bcoll, j.gozalvez}@umh.es

**Abstract**—The 5G New Radio (NR) Vehicle-to-Everything (V2X) Sidelink (SL) standard defines multiple DeModulation Reference Signal (DMRS) patterns to support direct vehicular communications in high mobility scenarios. The DMRS pattern is a pre-defined sequence of signals that can be adapted for the transmission of each Transport Block (TB), and is used to estimate the channel response and mitigate the impact of the Doppler shifts experienced by the received signal in high relative speed conditions. The standard defines multiple DMRS patterns, but it does not provide any recommendations to indicate when each pattern should be used. To this end, this study presents an exhaustive analysis of the impact that the DMRS patterns have on the link level performance of NR V2X SL communications, deriving the first set of NR V2X SL recommendations on the DMRS pattern selection. The recommendations identify the maximum Modulation and Coding Scheme (MCS) that can be supported by each DMRS pattern to ensure high reliability levels, and cover different relative speeds, propagation scenarios, and number of subchannels. We also openly release the link level results generated and analysed in this study to derive the recommendations. To the authors' knowledge, the obtained results represent the largest NR V2X SL link level dataset openly available.

**Keywords**—V2X, NR V2X, 5G, SL, Sidelink, DMRS, Doppler, link level, open, dataset.

## I. INTRODUCTION

Vehicle-to-Everything (V2X) connectivity will play a crucial role in the digital transformation of transportation into a cooperative ecosystem where road users can exchange the information needed for a more sustainable, efficient, and safe mobility. To this end, 3GPP introduced New Radio (NR) V2X Sidelink (SL) communications [1] to allow connected vehicles to directly exchange information between each other (Vehicle-to-Vehicle, V2V), with infrastructure nodes, and with vulnerable road users to support safety-critical applications without depending on the network coverage. The 5G NR V2X SL standard introduces a flexible Medium Access Control (MAC) and Physical (PHY) layer to cope with the wide range of latency and reliability requirements that connected and automated driving use cases exhibit [2]. At the PHY layer, NR V2X SL supports multiple SubCarrier Spacing (SCS) configurations, more spectrally efficient Modulation and Coding Schemes (MCSs), and a dedicated set of DeModulation Reference Signal (DMRS) patterns for the Physical Sidelink Control Channel (PSCCH) and for the Physical Sidelink Shared Channel (PSSCH), i.e., the PHY layer channels for the transmission of control and data information, respectively.

The DMRS patterns are a pre-defined sequence of signals used to estimate the channel response and correctly demodulate the received signals. The DMRS patterns can strongly influence the reliability of NR V2X SL communications in high-mobility scenarios where the received signal can experience large Doppler shifts under high transmitter-receiver relative speeds. This effect is highlighted

in [3] and [4], where the authors assess the robustness of the DMRS pattern defined for the PSCCH considering a wide range of Tx-Rx relative speeds.

The NR V2X SL standard defines a single and extremely robust DMRS pattern for the PSCCH channel, as it carries critical control information for the correct decoding of the TBs. On the other hand, the standard defines multiple DMRS patterns for the PSSCH that offer a trade-off between Link Level (LL) robustness and transmission efficiency, as the selection of more robust DMRS patterns reduces the maximum Transport Block (TB) size that can be transmitted in a subchannel. The selection of the PSSCH DMRS pattern can be adapted on a per packet (or TB) basis, but few studies have analysed the impact of the PSSCH DMRS patterns on the LL reliability of NR V2X SL communications. For example, the 3GPP pre-standardization studies in [5] and [6] analysed the LL PSSCH performance considering a single channel model and a restricted set of MCSs, namely QPSK-0.3 and 64QAM-0.5, and QPSK-0.5, respectively. However, they considered a single DMRS pattern that was ultimately not included in the standardized NR V2X SL specifications.

This study progresses the state-of-the-art with an in-depth evaluation of the impact that the different DMRS patterns defined for the PSSCH have on the LL performance of NR V2X SL communications. The LL performance analysis considers an exhaustive set of Block Error Rate (BLER) vs Signal-to-Noise Ratio (SNR) curves that cover over 3800 combinations of NR V2X SL parameters and scenarios. The study has been conducted using a LL simulator developed by the authors that is fully aligned with NR V2X SL specifications and is openly available at [7]. We also openly release the 3800+ BLER vs SNR curves generated and analysed in this study at [8]. To the authors' knowledge, the obtained results represent the largest NR V2X SL LL dataset openly available in the community. In addition, we leverage the LL evaluation to derive the first set of recommendations on the PSSCH DMRS pattern selection in NR V2X SL communications. The recommendations identify the maximum MCS that can be supported by each DMRS pattern to guarantee high reliability levels in line with the connected and automated driving use cases requirements defined in [2]. The recommendations on the DMRS pattern selection represent a valuable asset for the community, as they provide relevant indications for the robust and efficient configuration of the NR V2X SL PHY layer. The recommendations cover all channel models defined by 3GPP evaluation guidelines for the highway and urban scenarios, a representative range of transmitter-receiver relative speeds, and different numbers of subchannels.

## II. NR V2X SL PHYSICAL LAYER

NR V2X SL radio resources are organized on a time-frequency grid that can be flexibly configured based on the OFDM numerology ( $\mu$ ). In the time domain, resources are organized into 1 ms subframes with  $2^\mu$  time slots in each subframe. The duration of a time slot is  $2^{-\mu}$  ms and a time slot

contains 14 OFDM symbols. In the frequency domain, resources are organized into Resource Blocks (RBs). An RB is made of 12 adjacent OFDM subcarriers separated by a SubCarrier Spacing (SCS) of  $2^\mu \times 15$  kHz. NR V2X SL operates in the frequency range 1 (410 MHz – 7.125 GHz) where the value of  $\mu$  can be set to 0, 1, or 2. When  $\mu = \{0, 1, 2\}$ , the number of time slots in a single 1 ms subframe is  $\{1, 2, 4\}$  and the supported SCS values are  $\{15, 30, 60\}$  kHz.

A group of  $M_{sub}$  consecutive RBs within a time slot forms a subchannel. The size of a subchannel ( $M_{sub}$ ) can be equal to 10, 12, 15, 20, 25, 50, 75, or 100 RBs [9]. In NR V2X SL, the subchannel is the smallest PHY layer unit for the transmission and reception of the PSSCH and the PSCCH. The PSCCH is the PHY layer channel used to transmit the TB and the 2<sup>nd</sup>-stage Sidelink Control Information (SCI). The TB includes the message payload and can be transmitted using one of the MCSs reported in [10] (from Table 5.1.3.1-1 to Table 5.1.3.1-3). The 2<sup>nd</sup>-stage SCI carries control information needed to support retransmissions and multiple communication modes (unicast, groupcast, or broadcast), and is always transmitted using QPSK modulation. The PSCCH transmits the 1<sup>st</sup>-stage SCI, which contains relevant information for the correct decoding of the associated TB (e.g., the employed MCS). The 1<sup>st</sup>-stage SCI is transmitted using QPSK modulation with a high redundancy code rate.

In NR V2X SL, the PSSCH and PSCCH are multiplexed on non-overlapping Resource Elements (REs) within the same subchannel(s) [10]. A RE consists of a single subcarrier within an OFDM symbol. The PSCCH is allocated on the lowest RBs of the first subchannel utilized for the NR V2X SL transmission, and it can occupy 2 or 3 OFDM symbols starting from the 2<sup>nd</sup> symbol of the slot. The number  $M_{PSCCH}$  of RBs utilized by the PSCCH can be 10, 12, 15, 20, or 25, as long as  $M_{PSCCH} \leq M_{sub}$  [10].

NR V2X SL defines distinct DMRS patterns for the PSSCH and the PSCCH. DMRS patterns are pre-defined sequences of signals used by the receiver to estimate the radio channel response and correctly demodulate the received signals. The amount of DMRSs transmitted within a single slot, as well as the DMRS's position within the slot, can strongly influence the robustness of NR V2X SL communications against frequency and time selective fading, especially under the presence of large Doppler shifts that reduce the channel's coherence time. In this context, the PSSCH supports multiple DMRS patterns with different robustness levels.

The DMRS patterns defined for the PSSCH can consist of a variable number of OFDM symbols ( $N_{DMRS}$ ), where  $N_{DMRS}$  can be equal to  $\{2, 3, 4\}$  [11]. The PSSCH DMRS patterns supported by the NR V2X SL PHY layer are illustrated in Fig. 1 when the number of subchannels ( $N_{sub}$ ) employed for NR V2X SL transmissions is equal to one and larger than one, assuming that the PSCCH occupies 3 OFDM symbols and  $M_{PSCCH} = M_{sub}$ . We should note that, when  $N_{sub}$  is larger than 1, the total number of RBs occupied for the NR V2X SL transmissions is equal to  $N_{sub} \cdot M_{sub}$ . Fig. 1(a) and Fig. 1(b) illustrate the position of the PSSCH DMRS pattern symbols when  $N_{DMRS}$  is equal to 2 considering  $N_{sub} = 1$  and  $N_{sub} > 1$ , respectively<sup>1</sup>. Fig. 1(c) and Fig. 1(d) represent the PSSCH DMRS pattern when  $N_{DMRS}$  is equal to 3 and 4 and  $N_{sub} > 1$ . Fig. 1(c) and Fig. 1(d) show that the PSSCH DMRS patterns

with  $N_{DMRS} = \{3, 4\}$  multiplex the PSSCH DMRSs and the PSCCH on adjacent REs within the second OFDM symbol. In the  $N_{sub} = 1$  case, such multiplexing is only supported if  $M_{sub} \geq 20$  RBs according to the standard (Section 8.2.2 of [10]). When  $M_{sub} < 20$  RBs, only the PSSCH DMRS pattern with  $N_{DMRS} = 2$  illustrated in Fig. 1(a) can be employed. We should note that the PSSCH DMRSs occupy one every two REs on the OFDM symbols where the PSSCH DMRS is transmitted (Section 8.4.1.2.2 of [11]). The REs that are not utilized for the transmission of the PSSCH DMRSs are utilized to transmit the PSSCH.

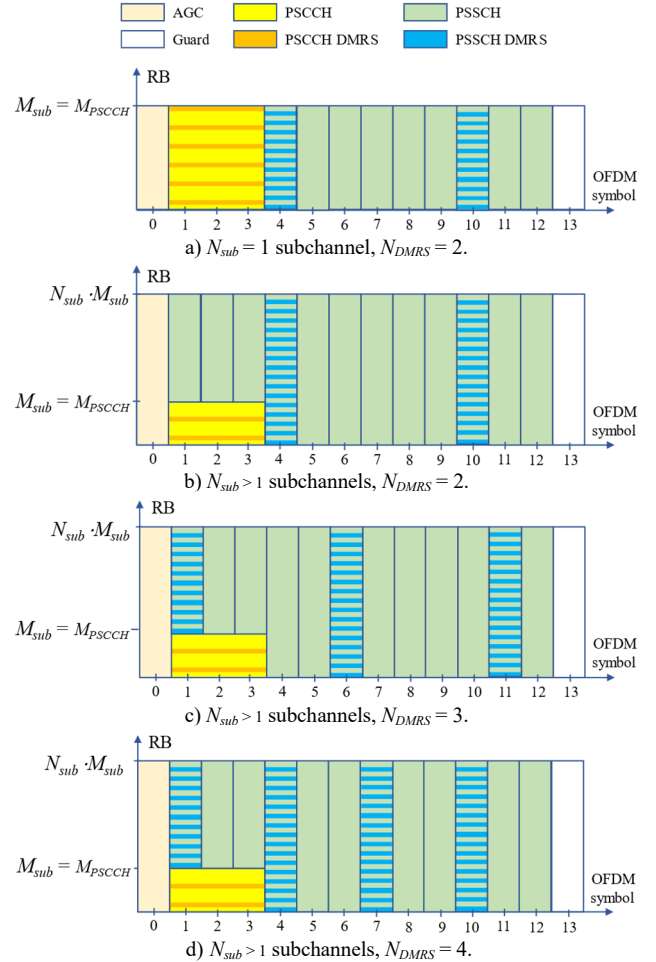


Fig. 1. DMRS patterns in NR V2X SL.

The PSCCH carries important information for correctly decoding the associated TB and, for this reason, is protected with a fixed and very robust DMRS pattern. Within the time-frequency resources occupied by the PSCCH, the PSCCH DMRSs are placed every 4 REs. The PSCCH is transmitted in the REs that are not utilized to accommodate the PSCCH DMRSs. In the remainder of this work, we concentrate on the DMRS patterns defined for the PSSCH and, for the sake of brevity, we refer to the PSSCH DMRS patterns as DMRS patterns.

### III. NR V2X SL LINK LEVEL SIMULATOR

This work analyses the impact of the DMRS patterns on the PHY layer performance of NR V2X SL using a NR V2X SL

<sup>1</sup> Note that the first OFDM symbol within a slot is used for Automatic Gain Control (AGC) purposes while the last one is a guard symbol to allow the

switching between the Tx and Rx mode. The AGC symbol is filled with a copy of the second OFDM symbol, whereas the guard symbol is left empty.

LL simulator developed by the authors using Matlab’s 5G toolbox (version R2022a). The simulator is openly available at [7] and features a standard-compliant implementation of the NR V2X SL PHY layer that includes the transmitter/receiver chains and V2V sidelink channel models.

The transmitter chain of the NR V2X SL LL simulator includes all the modules needed for the encoding, multiplexing, modulation, and transmission of the TBs and the associated SCIs. The transmitter chain is also responsible for the generation of the DMRS patterns. The DMRS pattern signals are generated using a pseudo-random sequence that is initialized using the decimal representation of the 1<sup>st</sup>-stage SCI Cyclic Redundancy Check (CRC). The simulator implements all the DMRS patterns reported in NR V2X SL specifications and introduced in Section II.

The simulator also implements the V2V Clustered Delay Line (CDL) channel models defined by 3GPP evaluation guidelines in [12] to model the small-scale fading effects that characterize NR V2X SL communications under different Line-of-Sight (LOS) propagation conditions in the Highway and Urban environments. The LOS channel models represent a V2V link with a direct transmitter-receiver LOS path. The NLOSv channel models assume that the direct transmitter-receiver LOS path is blocked by the presence of other vehicles. LOS and NLOSv models are available for both the Highway and Urban environments. The urban environment also includes a NLOS channel model to capture the channel characteristics when the V2V link is blocked by the presence of buildings. It is important to highlight that each channel model can be customized with specific Doppler shift configurations to model the impact of different Tx-Rx relative speed values.

The receiver chain processes the channel-impaired waveform captured by each of the receiving antennas. Its main functionalities are: timing and channel estimation, equalization, demodulation, demultiplexing, and decoding. Timing and channel estimation rely on the DMRS patterns to estimate the distortions introduced by the V2V CDL channel and guarantee an accurate equalization of the received signal. Equalization is performed using the Minimum Mean Square Error (MMSE) algorithm. We should note that, as PSSCH and PSCCH employ different DMRS patterns, they undergo separate timing estimation, channel estimation, and equalization operations on two parallel branches of the receiver chain. Additional details on the NR V2X SL link level simulator are available in [13] and the code can be downloaded from [7].

#### IV. NR V2X SL CONFIGURATION

The flexible design of NR V2X SL communications is characterized by the availability of a large number of configurable parameters. To this end, 3GPP and ETSI working groups have identified a default set of NR V2X SL parameters in [12] and [14] to define a common reference NR V2X SL configuration. The definition of a default set of NR V2X SL parameters is important for two reasons. First, it provides connected vehicles a common NR V2X SL configuration for direct V2V communications without the support or intervention of the cellular infrastructure. Second, it establishes a common evaluation framework for the assessment of NR V2X SL performance.

TABLE I  
DEFAULT NR V2X SL PARAMETERS SET.

Parameter	Value
A) 3GPP fixed parameters [12].	
Operating frequency	5.9 GHz
Number of Tx-Rx antennas	2 Tx 4 Rx
Antenna type	Isotropic
Number of Tx layers	1
B) 3GPP configurable parameters [12].	
Channel models, Highway	{LOS, NLOSv}
Channel models, Urban	{LOS, NLOS, NLOSv}
$v_{rel}$ , Highway	{0, 70, 140, 280} km/h
$v_{rel}$ , Urban	{0, 60, 120} km/h
C) ETSI fixed parameters [14].	
Bandwidth	20 MHz
Subcarrier spacing	30 kHz
OFDM symbols per slot	14
Subchannel size	10 RBs
Available subchannels	5
PSCCH RBs	10 RBs
PSCCH OFDM symbols	3
PSSCH DMRS Pattern, $N_{DMRS}$	{2, 3, 4}
D) ETSI configurable parameters [14].	
MCS	28 possible MCSs from Table 5.1.3.1-2 [10]
Number of subchannels $N_{sub}$	{1, 2, 3, 4, 5}

Table I reports the default NR V2X SL fixed and configurable parameters provided by 3GPP and ETSI. 3GPP-defined parameters include the operating frequency, the number of Tx and Rx antennas, the channel models, and the Tx-Rx relative speed ( $v_{rel}$ ) values for the Highway and Urban environments. ETSI provides a default configuration for all the Radio Resource Control (RRC), Radio Link Control (RLC), MAC, and PHY layer parameters that characterize the NR V2X SL protocol stack. For example, ETSI establishes default values for the recommended channel bandwidth, subcarrier spacing, subchannel size, MCS (ranging from QPSK-120 to 256QAM-948), and DMRS pattern. However, ETSI does not identify a specific DMRS pattern. Instead, it reports the complete set of DMRS patterns defined by the NR V2X SL standard, hence leaving the selection of the DMRS pattern up to each implementation. In this regard, this paper presents an in-depth analysis of the DMRS patterns to identify the most adequate DMRS pattern under a large variety of operating conditions, including propagation environments and Tx-Rx relative speeds.

#### V. NUMERICAL RESULTS

This section evaluates the impact of the DMRS patterns on the LL performance of NR V2X SL communications. The LL performance is reported in the form of BLER vs SNR curves that have been obtained by varying the average SNR. The average SNR is a configurable parameter of the NR V2X SL link level simulator employed in this work. For each SNR value, we measured the BLER as the fraction of incorrectly received TB transmissions with respect to the total. We simulated a sufficiently large number of transmissions to ensure the statistical accuracy of the results. We focus the presentation of numerical results on the Highway environment since it is characterized by the largest Tx-Rx relative speed values, hence representing the most challenging scenario for the DMRS-based channel estimation mechanism employed in NR V2X SL. However, we have evaluated the LL performance considering all possible combinations of the

configurable parameters included in Table I, obtaining a total of 3808 BLER vs SNR curves. These curves are openly released at [8] and represent, to the authors' knowledge, the largest NR V2X SL link level dataset openly available in the community.

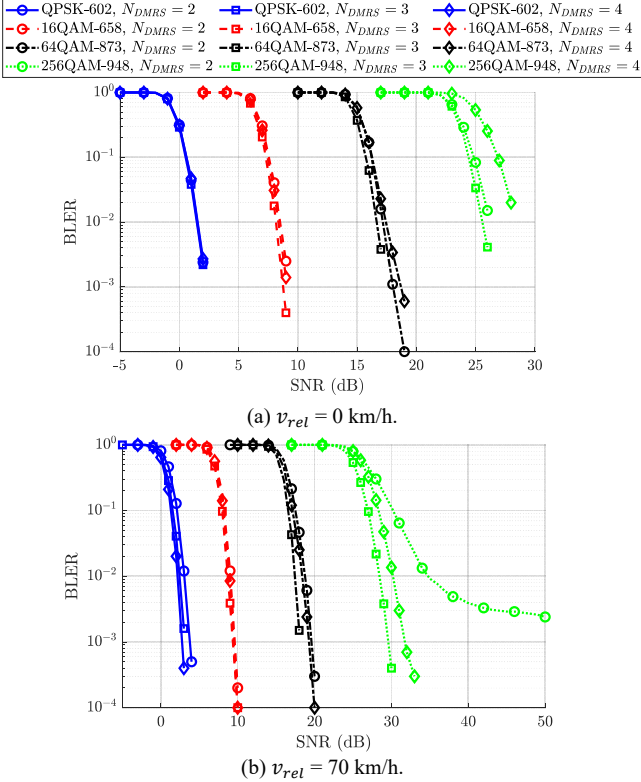


Fig. 2. Impact of the DMRS pattern on the NR V2X SL link level performance for  $v_{rel} = 0$  km/h and  $v_{rel} = 70$  km/h.

Fig. 2 reports the impact of the DMRS patterns on the LL performance considering the Highway-LOS scenario,  $N_{sub} = 2$ , two relative speed values, i.e.,  $v_{rel} = 0$  km/h and  $v_{rel} = 70$  km/h, and a selected set of MCSs, namely QPSK-602, 16QAM-658, 64QAM-873, and 256QAM-948. These MCS represent the highest code rate configuration for each modulation scheme included in the default NR V2X SL parameters set. They correspond to MCS index ( $I_{MCS}$ ) 4, 10, 19, and 27 in Table 5.1.3.1-2 [10]. For  $v_{rel} = 0$  km/h, Fig. 2(a) shows that the LL performance is not significantly influenced by the adoption of more robust DMRS patterns with  $N_{DMRS}$  equal to 3 or 4. This is the case because the relative speed and resulting Doppler shift are small, and the DMRS pattern with  $N_{DMRS} = 2$  is sufficiently robust to guarantee a correct channel estimation and equalization process. Fig. 2(a) shows that it is possible to correctly decode all received packets (i.e., BLER = 0) under sufficiently large SNR values for all the considered MCSs and DMRS patterns. However, Fig. 2(a) uses a logarithmic scale and, therefore, BLER values equal to zero cannot be reported. Fig. 2(a) reports the LL results obtained for the MCS with the highest code rate (i.e., with the lowest error protection) of each modulation order. Therefore, it is possible to conclude that the DMRS pattern with  $N_{DMRS} = 2$  is sufficient to guarantee a reliable link level performance when  $v_{rel} = 0$  km/h. This is not necessarily the case in the  $v_{rel} = 70$  km/h setting analysed in Fig. 2(b). Fig. 2(b) shows that the use of a DMRS pattern with  $N_{DMRS}$  equal to 2 results in an error floor for the 256QAM-948 MCS ( $I_{MCS} = 27$ ), indicating that the correct decoding of all received TBs cannot be guaranteed, regardless of the SNR value. However, we focus our link level

analysis on the 99% reliability level (i.e., a BLER of  $10^{-2}$ ) identified by the service requirements analysis for connected and automated driving presented by ETSI and 3GPP in [2]. In this regard, the DMRS pattern with  $N_{DMRS} = 2$  can meet the 99% reliability target also in the 256QAM-948 case when  $v_{rel} = 70$  km/h, although it provides a lower reliability than the DMRS patterns with  $N_{DMRS} = 3$  or  $N_{DMRS} = 4$ .

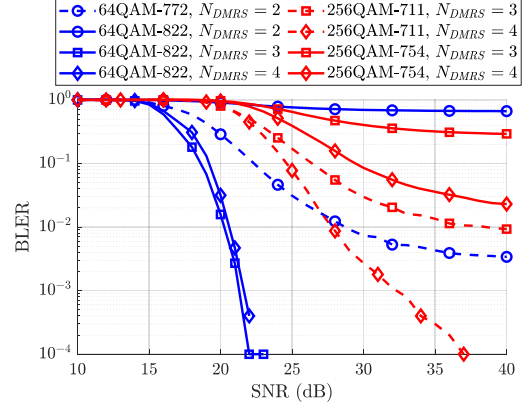


Fig. 3. Impact of the DMRS pattern on the NR V2X SL link level performance,  $v_{rel} = 140$  km/h.

Fig. 3 depicts the link level performance when  $v_{rel} = 140$  km/h under the same simulation assumptions of Fig. 2 (Highway LOS channel,  $N_{sub} = 2$ ). Fig. 3 shows that the DMRS pattern with  $N_{DMRS} = 2$  can only guarantee a 99% reliability up to the MCS 64QAM-772 ( $I_{MCS} = 17$ ). 64QAM-822 ( $I_{MCS} = 18$ ) and more spectrally efficient (i.e., less robust) MCSs exhibit an error floor above the  $10^{-2}$  BLER threshold when  $N_{DMRS} = 2$ . These MCSs require the use of the DMRS patterns with  $N_{DMRS}$  equal to 3 and 4 when  $v_{rel} = 140$  km/h. However, Fig. 3 shows that both the DMRS pattern with  $N_{DMRS}$  equal to 3 and 4 can only meet the 99% reliability up to the 256QAM-711 MCS ( $I_{MCS} = 21$ ). The DMRS pattern with  $N_{DMRS} = 4$  is more robust than its counterpart with  $N_{DMRS} = 3$  and achieves a better BLER. However, it is not able to guarantee an error floor below the  $10^{-2}$  BLER threshold for the MCSs that are more spectrally efficient than 256QAM-711, e.g., the 256QAM-754 MCS ( $I_{MCS} = 22$ ) reported in Fig. 3.

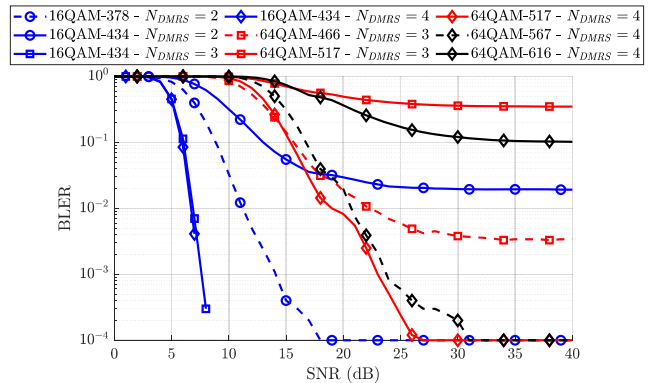


Fig. 4. Impact of the DMRS pattern on the NR V2X SL link level performance,  $v_{rel} = 280$  km/h.

Fig. 4 represents the NR V2X SL link level performance with  $v_{rel} = 280$  km/h in the Highway LOS scenario with  $N_{sub} = 2$ . In this case, the  $N_{DMRS} = 2$  DMRS pattern can only guarantee a 99% reliability (i.e., a BLER below the  $10^{-2}$  threshold) up to the 16QAM-378 MCS ( $I_{MCS} = 5$ ). 16QAM-434 ( $I_{MCS} = 6$ ) and more spectrally efficient MCSs exhibit an

error floor above the  $10^{-2}$  threshold; for example, the maximum reliability that the 16QAM-434 MCS can achieve with  $N_{DMRS} = 2$  is 98% since this MCS exhibits an error floor at BLER = 0.02. From the 16QAM-434 MCS, it is necessary to use more robust DMRS patterns with  $N_{DMRS}$  equal to 3 and 4 to cope with the large Doppler shifts that characterize the  $v_{rel} = 280$  km/h scenario. When  $N_{DMRS} = 3$ , Fig. 4 shows that it is possible to achieve a 99% reliability up to the MCS 64QAM-466 ( $I_{MCS} = 11$ ). If we further reduce the error protection and employ MCSs from 64QAM-517 ( $I_{MCS} = 12$ ), the DMRS pattern with  $N_{DMRS} = 3$  cannot meet the 99% reliability requirement, and it is necessary to use the  $N_{DMRS} = 4$  configuration, as it is the only DMRS pattern that can achieve a BLER below  $10^{-2}$ . However, this DMRS pattern is also not able to guarantee a 99% reliability for all MCSs included in the default NR V2X SL parameters set despite being the most robust. Fig. 4 shows that the most spectrally efficient MCS (i.e., the one with the highest MCS index) that meets the 99% reliability requirement when using the  $N_{DMRS} = 4$  DMRS pattern is 64QAM-567 ( $I_{MCS} = 13$ ). From 64QAM-616 ( $I_{MCS} = 14$ ), none of the NR V2X SL DMRS patterns is able to guarantee a 99% reliability.

Fig. 2 to Fig. 4 demonstrated the impact of the DMRS pattern on the LL performance of NR V2X SL communications. The results show that more robust DMRS patterns are necessary to guarantee a high reliability when the Tx-Rx relative speed increases. Fig. 2 to Fig. 4 are obtained considering the Highway LOS scenario, but similar trends are observed in the Highway NLOSv case and also in the Urban LOS, NLOSv, and NLOS scenarios. In this study, we leverage the obtained NR V2X SL link level results to identify the maximum MCS that can be supported by each DMRS pattern to guarantee a 99% reliability and provide recommendations on the selection of the DMRS pattern in NR V2X SL.

Table II summarizes the PHY layer recommendations defined for the Highway LOS and Highway NLOSv scenarios considering the  $N_{sub}$  and relative speed values included in the default NR V2X SL parameters set. We should note that only the  $N_{DMRS} = 2$  configuration is available for  $N_{sub} = 1$  in Table II (see Section II). The table identifies, for each scenario, the maximum MCS that can be supported by each DMRS pattern to guarantee a 99% reliability. Table II shows that the number of occupied subchannels ( $N_{sub}$ ) has an impact on the PHY layer recommendations for the higher relative speeds ( $v_{rel} = 140, 280$  km/h). For example, the maximum MCS supported by the  $N_{DMRS} = 2$  DMRS pattern in the Highway LOS scenario decreases from 64QAM-873 ( $I_{MCS} = 19$ ) and 16QAM-490 ( $I_{MCS} = 7$ ) to 64QAM-772 ( $I_{MCS} = 17$ ) and 16QAM-378 ( $I_{MCS} = 5$ ) when moving from  $N_{sub} = 1$  to  $N_{sub} = 2$  in the 140 km/h and 280 km/h settings, respectively. Similar trends are observed in the Highway NLOSv case. Moreover, Table II reveals that the maximum MCS supported by each DMRS pattern can depend on the propagation scenario too. For instance, the maximum MCS supported by the  $N_{DMRS} = 3$  pattern with  $v_{rel} = 280$  km/h and  $N_{sub} = 3$  increases from 16QAM-658 ( $I_{MCS} = 10$ ) to 64QAM-517 ( $I_{MCS} = 12$ ) when moving from the Highway LOS to the Highway NLOSv scenario. This is the case because the large Doppler spreads experienced with high relative speeds (140 km/h and 280 km/h) provide another means for diversity that can be exploited to improve the channel estimation and equalization

process, as demonstrated in [15]. The improvements resulting from such additional diversity increase with the number of multipath components, and the NLOSv channel has a larger number of multipath components than the LOS channel (see CDL channels definition in [12])<sup>2</sup>.

TABLE II  
PHY LAYER RECOMMENDATIONS, HIGHWAY SCENARIO.

Channel model	$v_{rel}$ [km/h]	$N_{sub}$	$N_{DMRS}$	Max MCS ( $I_{MCS}$ )	
Highway LOS	0, 70	1, 2, 3, 4, 5	2, 3, 4	256QAM-948 (27)	
			1	2	64QAM-873 (19)
	140	1	2	64QAM-772 (17)	
			3, 4	256QAM-711 (21)	
		2	2	64QAM-616 (14)	
			3, 4	256QAM-682.5 (20)	
		3	2	64QAM-616 (14)	
			3, 4	256QAM-682.5 (20)	
		4	2	64QAM-616 (14)	
			3, 4	256QAM-682.5 (20)	
		5	2	64QAM-616 (14)	
			3, 4	256QAM-682.5 (20)	
	280	1	2	16QAM-490 (7)	
			2	16QAM-378 (5)	
		2	3	64QAM-466 (11)	
			4	64QAM-567 (13)	
		3, 4	2	16QAM-378 (5)	
			3	16QAM-658 (10)	
		4	2	64QAM-466 (11)	
			3, 4	64QAM-466 (11)	
5		2	QPSK-602 (4)		
		3, 4	64QAM-466 (11)		
Highway NLOSv	0, 70	1, 2, 3, 4, 5	2, 3, 4	256QAM-948 (27)	
			1	2	64QAM-873 (19)
	140	1	2	64QAM-719 (16)	
			3	256QAM-711 (21)	
		2	4	256QAM-754 (22)	
			2	64QAM-719 (16)	
		3	3, 4	256QAM-711 (21)	
			2	64QAM-616 (14)	
		4, 5	3, 4	256QAM-711 (21)	
			2	16QAM-553 (8)	
		280	1	2	16QAM-434 (6)
				3	64QAM-466 (11)
	2		4	64QAM-616 (14)	
			2	16QAM-434 (6)	
	3, 4		3, 4	64QAM-517 (12)	
			2	QPSK-602 (4)	
	5		3, 4	64QAM-466 (11)	

For the sake of completeness, Table III reports the PHY layer recommendations for the Urban scenario. Like in the Highway scenario, the maximum MCS supported by each DMRS pattern depends on the number of occupied subchannel and the channel model. The Urban scenario is characterized by smaller Tx-Rx relative speed values (up to 120 km/h), and each DMRS pattern is able to support a larger number of MCSs with respect to the Highway scenario. For example, the  $N_{DMRS} = 2$  DMRS pattern can support all MCSs up to 64QAM-666 ( $I_{MCS} = 15$ ) in the Urban LOS scenario, regardless of the Tx-Rx relative speed and the  $N_{sub}$  value. On the other hand, the maximum MCS supported by the  $N_{DMRS} = 2$  DMRS pattern is limited to QPSK-602 ( $I_{MCS} = 4$ ) in the Highway LOS scenario when  $v_{rel} = 280$  km/h.

<sup>2</sup>Nevertheless, we should note that the average SNR at a given Tx-Rx distance is smaller for the NLOSv scenario than the LOS scenario due to its more severe pathloss and shadowing.



TABLE III  
PHY LAYER RECOMMENDATIONS, URBAN SCENARIO.

Channel model	$v_{rel}$ [km/h]	$N_{sub}$	$N_{DMRS}$	Max MCS ( $I_{MCS}$ )	
Urban LOS	0, 60	1, 2, 3, 4, 5	2, 3, 4	256QAM-948 (27)	
		1	2	256QAM-711 (21)	
	120	2	2	64QAM-822 (18)	
			3	256QAM-754 (22)	
			4	256QAM-797 (23)	
		3	2	64QAM-719 (16)	
			3, 4	256QAM-754 (22)	
		4, 5	2	64QAM-666 (15)	
	3, 4	256QAM-754 (22)			
	Urban NLOSv	0, 60	1, 2, 3, 4, 5	2, 3, 4	256QAM-948 (27)
1			2	256QAM-711 (21)	
120		2	2	64QAM-822 (18)	
			3	256QAM-754 (22)	
			4	256QAM-797 (23)	
		3	2	64QAM-772 (17)	
			3	256QAM-754 (22)	
			4	256QAM-797 (23)	
4		2	64QAM-772 (17)		
		3, 4	256QAM-797 (23)		
		5	64QAM-719 (16)		
3, 4		256QAM-754 (22)			
Urban NLOS		0, 60	1, 2, 3, 4, 5	2, 3, 4	256QAM-948 (27)
			1	2	256QAM-841 (24)
		120	2	2	256QAM-797 (23)
				3, 4	256QAM-916.5 (26)
				2	256QAM-711 (21)
			3	3, 4	256QAM-916.5 (26)
	2			256QAM-682.5 (20)	
	3, 4		256QAM-916.5 (26)		
	4	2	256QAM-682.5 (20)		
		3, 4	256QAM-682.5 (20)		
	5	2	256QAM-682.5 (20)		
	3, 4	256QAM-885 (25)			

The previous results have demonstrated that DMRS patterns with a larger  $N_{DMRS}$  value improve the channel estimation accuracy and guarantee a more robust LL performance. However, more robust DMRS patterns reduce the maximum TB size (TBS) that can be transmitted over a given number of subchannels. This is the case since the PSSCH can be transmitted only on the REs that are not occupied by the PSSCH DMRSs (see Section II). Table IV illustrates the impact of the DMRS pattern on the TBS considering two occupied subchannels ( $N_{sub} = 2$ ) and the four MCS configurations of Fig. 2. Table IV shows that the selection of a DMRS pattern with  $N_{DMRS} = 3$  and  $N_{DMRS} = 4$  can reduce the TB size by up to 4.4% and 8.8% with respect to the  $N_{DMRS} = 2$  configuration. The trade-off between communication robustness and transmission efficiency is an important aspect that should not be neglected when selecting the DMRS pattern.

## VI. CONCLUSIONS

This study has analysed the impact of the DMRS patterns defined for the PSSCH on the link level performance of NR V2X SL communications. The link level analysis has been leveraged to derive the first set of recommendations on the PHY layer configuration of NR V2X SL communications. The recommendations identify the maximum MCS that can be supported by each DMRS pattern to provide high reliability levels. The study has also demonstrated the trade-off between communication robustness and transmission efficiency that characterizes the DMRS pattern selection, as more robust patterns reduce the maximum TB size that can be transmitted per subchannel. Numerical results were shown for the Highway scenario, but we also presented the complete set of PHY layer recommendations for the Highway and Urban

scenarios that cover all possible combinations of configurable parameters included in the default set of NR V2X SL parameters. We openly release at [8] the 3808 BLER vs SNR curves generated and analysed in this study. To the authors' knowledge, the obtained results represent the largest NR V2X SL link level dataset openly available in the community.

TABLE IV  
IMPACT OF THE DMRS PATTERN ON THE TB SIZE,  $N_{sub} = 2$ .

MCS	$N_{DMRS}$	TBS [B]	Reduction
QPSK-602	2	325	-
	3	317	2.5%
	4	301	7.3%
16QAM-658	2	720	-
	3	688	4.4%
	4	656	8.8%
64QAM-873	2	1441	-
	3	1377	4.4%
	4	1313	8.8%
256QAM-948	2	2049	-
	3	2017	1.5%
	4	1921	6.2%

## ACKNOWLEDGEMENTS

This work was supported in part by Generalitat Valenciana and MCIU/AEI/10.13039/501100011033 (grant no. PID2020-115576RB-I00). The work of Luca Lusvardi was also supported by the European Union under the 2023 MSCA Postdoctoral Fellowship program (project no. 101153845). The authors would also like to acknowledge Pasquale Di Viesti (UniMoRe), Thomas Jacobsen (NOKIA), and Renato Abreu (NOKIA) for their valuable suggestions and feedback.

## REFERENCES

- [1] 3GPP, "TR 21.916 Release 16 Description; Summary of Rel-16 Work Items (v16.2.0, Release 16)," 3GPP, Tech. Report, July 2022.
- [2] 3GPP, "TS 22.186 5G; Service requirements for enhanced V2X scenarios (v16.2.0, Release 16)," 3GPP, Tech. Spec., Nov. 2020.
- [3] S.-Y. Lien *et al.*, "3GPP NR Sidelink Communications Toward 5G V2X," *IEEE Access*, vol. 8, pp. 35368-35382, 2020.
- [4] 3GPP, "Link level evaluations of NR PSSCH," R1-1903180, 3GPP TSG-RAN WG1 Meeting #96, March 2019.
- [5] 3GPP, "Sidelink physical layer structure for NR V2X," R1-1911882, 3GPP TSG RAN WG1 Meeting #99, Nov. 2019.
- [6] 3GPP, "Link level evaluations of NR PSSCH," R1-1903181, 3GPP TSG-RAN WG1 Meeting #96, March 2019.
- [7] GitHub repository of the NR V2X SL Link Level simulator: <https://github.com/uwicore/NR-V2X-SL-LinkLevelSimulator>.
- [8] *NR V2X SL link-level repository*, UWICORE Research Laboratory, Universidad Miguel Hernandez de Elche, April 2024. [Online]. Available: <https://uwicore.umh.es/NRV2XSL-LinkLevel.html>
- [9] 3GPP, "TS 38.331 NR; Radio Resource Control (RRC); Protocol Specification (v17.7.0, Release 17)," 3GPP, Tech. Spec., Feb. 2024.
- [10] 3GPP, "TS 38.214 NR; Physical layer procedures for data (v17.9.0, Release 17)," 3GPP, Tech. Spec., April 2024.
- [11] 3GPP, "TS 38.211 NR; Physical channels and modulation (v17.7.0, Release 17)," 3GPP, Tech. Spec., April 2024.
- [12] 3GPP, "TR 37.885; Study on evaluation methodology of new Vehicle-to-Everything (V2X) use cases for LTE and NR (v15.3.0, Release 15)," 3GPP, Tech. Rep., June 2019.
- [13] L. Lusvardi, B. Coll-Perales, J. Gosalvez and M. L. Merani, "Link Level Analysis of NR V2X Sidelink Communications," in *IEEE Internet of Things Journal*, Early Access.
- [14] ETSI, "LTE-V2X and NR-V2X Access layer specification for Intelligent Transport Systems operating in the 5 GHz frequency band; Release 2" ETSI EN 303 798 V 2.0.1, Oct. 2023.
- [15] A. M. Sayeed and B. Aazhang, "Joint multipath-Doppler diversity in mobile wireless communications," in *IEEE Transactions on Communications*, vol. 47, no. 1, pp. 123-132, Jan. 1999.